JOC The Journal of Organic Chemistry

ARTICLE

pubs.acs.org/joc

Synthesis, Structure, and Properties of Supramolecular Charge-Transfer Complexes between Bis(18-crown-6)stilbene and Ammonioalkyl Derivatives of 4,4′-Bipyridine and 2,7-Diazapyrene

Artem I. Vedernikov,[†] Evgeny N. Ushakov,[‡] Asya A. Efremova,[†] Lyudmila G. Kuz'mina,[§] Anna A. Moiseeva,[¶] Natalia A. Lobova,[†] Andrei V. Churakov,[§] Yuri A. Strelenko,[∥] Michael V. Alfimov,[†] Judith A. K. Howard,[⊥] and Sergey P. Gromov*[,†]

[†]Photochemistry Center, Russian Academy of Sciences, ul. Novatorov 7A-1, Moscow 119421, Russian Federation

[‡]Institute of Problems of Chemical Physics, Russian Academy of Sciences, Chernogolovka 142432, Moscow Region, Russian Federation

[§]N. S. Kurnakov Institute of General and Inorganic Chemistry, Russian Academy of Sciences, Leninskiy prosp. 31, Moscow 119991, Russian Federation

[¶]Chemistry Department, M. V. Lomonosov Moscow State University, Vorob'evy Gory, Moscow 119899, Russian Federation

[∥]N. D. Zelinskiy Institute of Organic Chemistry, Russian Academy of Sciences, Leninskiy prosp. 47, Moscow 119991, Russian Federation

[⊥]Chemistry Department, University of Durham, South Road, Durham DH1 3LE, U.K.

Supporting Information

ABSTRACT:

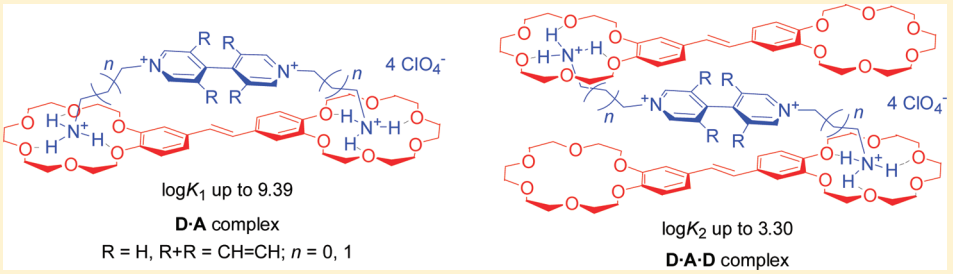

4,4′-Bipyridine and 2,7-diazapyrene derivatives (**A**) having two ammonioalkyl N-substituents were synthesized. The complex formation of these compounds with bis(18-crown-6)stilbene (**D**) was studied by spectrophotometry, cyclic voltammetry, ^{1}H NMR spectroscopy, and X-ray diffraction analysis. In MeCN, π-donor **D** and π-acceptors **A** form supramolecular 1:1 (**D**·**A**) and 2:1 (**D**·**A**·**D**) charge-transfer complexes. The **D**·**A** complexes have a pseudocyclic structure as a result of ditopic binding of the ammonium groups to the crown-ether fragments. The better the geometric matching between the components, the higher the stability of the **D**·**A** complexes (log K up to 9.39). A key driving force of the **D**·**A**·**D** complex formation is the excessive steric strain in the precursor **D**·**A** complexes. The pseudocyclic **D**·**A** complexes involving the ammoniopropyl derivative of 4,4′-bipyridine were obtained as single crystals. Crystallization of the related ammonioethyl derivative was accompanied by transition of the **D**·**A** complexes to a structure of the $(\mathbf{D}\cdot\mathbf{A})_m$ coordination polymer type.

INTRODUCTION

Organic donor−acceptor complexes, or charge-transfer (CT) complexes, play an important role in chemical and photochemical reactions,[1] in molecular self-assembly,[2] and in biological systems,[3] and they can be employed for organic photovoltaic devices and field-effect transistors.[4] In recent years, considerable attention has been paid to the synthesis and studies of supramolecular donor−acceptor systems in relation to their possible use as components of molecular electronic devices for solar energy conversion and sensor and catalytic applications.[5]

Previously,[6] we described supramolecular CT complexes between bis(18-crown-6)stilbene (*E*)-**1** and dipyridylethylene derivatives (*E*)-**2b,c**. Complexes [**1**·**2b,c**] are characterized by a very high thermodynamic stability, which is due to the ditopic binding of ammonium groups of acceptor **2** to the crown-ether fragments of donor **1**. It was shown that these complexes can act as fluorescence sensors for alkaline-earth metal ions.[6a] Moreover, they are very convenient model systems for investigation of ultrafast electron transfer reactions.[7]

In order to study the effect of the acceptor structure on the properties of supramolecular CT complexes such as [**1**·**2b,c**], we synthesized 4,4′-bipyridine derivatives **3b,c** and 2,7-diazapyrene derivatives **4b,c** containing two ammonioalkyl N-substituents.

Received: June 7, 2011
Published: July 11, 2011

Scheme 1. Structure of Acceptors 3a, 4a and Synthesis of Acceptors 3b,c and 4b,c

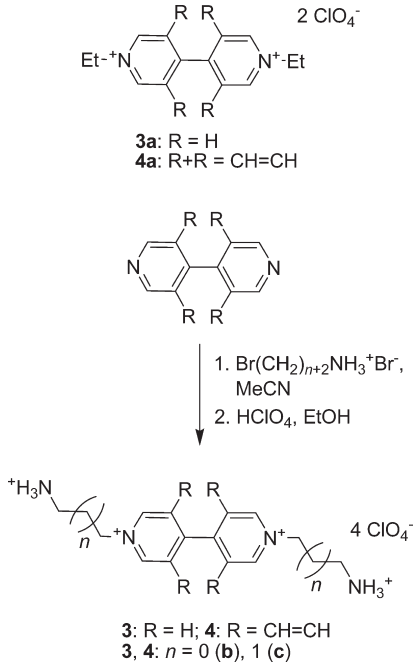

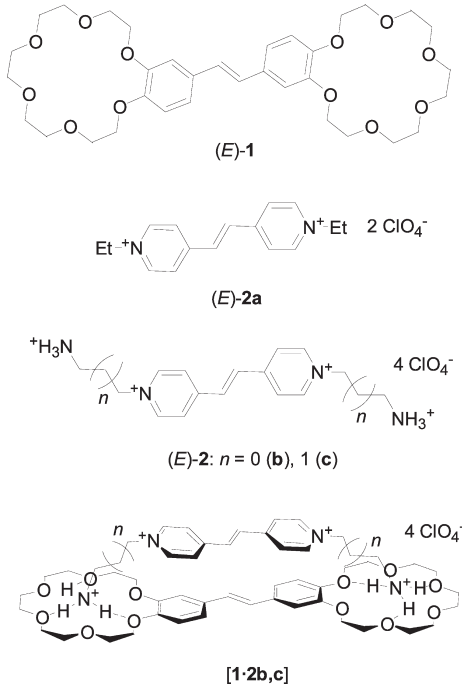

This paper gives an account of the studies of the structural features and the physicochemical properties of the complexes formed by these compounds with bis(crown)stilbene **1** in solutions and in the crystalline state. As model compounds, we used acceptors **3a** and **4a** devoid of ammonium groups.

RESULTS AND DISCUSSION

Synthesis. Previously,[8] we developed an efficient synthesis of symmetrical bis(crown)stilbenes, in particular (*E*)-**1**, consisting of the condensation of benzocrown ethers with 2-bromoacetaldehyde diethyl acetal in acid medium and subsequent rearrangement of the resulting 1,1-diaryl-2-bromoethanes to desired stilbenes. The synthesis of (*E*)-1,2-di(4-pyridyl)ethylene derivatives **2a**−**c** and model acceptor compounds **3a** and **4a** was described in our previous publications.[6a,9] Compounds **3b,c** and **4b,c** were prepared by quaternization of 4,4′-bipyridine and 2,7-diazapyrene with ω-bromoalkylammonium bromides in MeCN, followed by exchange of the anions with the perchlorates on treatment with concentrated $HClO_4$ in ethanol (Scheme 1).

Supramolecular complexes [**1**·**3b,c**] and [**1**·**4b,c**] were obtained as dark-colored fine-crystalline powders by slow precipitation from acetonitrile solutions of equimolar mixtures of components. The 1:1 formal stoichiometry was confirmed for these complexes by ^{1}H NMR spectroscopy, elemental analysis, and X-ray diffraction. It is noteworthy that repeated crystallization of the black-blue crystalline complex [**1**·**3b**] gave rise to almost colorless amorphous precipitate having the same stoichiometric composition. According to X-ray diffraction data (see below), in the crystalline complex [**1**·**3b**], effective CT interaction may occur between the π-donor and π-acceptor moieties, which is responsible for deep coloring. Probably, in the amorphous modification of [**1**·**3b**], the relative positions of these moieties are unfavorable for CT interactions and the complex components are thus connected only through hydrogen bonds.

CT Absorption Spectra and Complex Formation Constants. It has been demonstrated previously[6b,9b] that the complexation of bis(crown)stilbene (*E*)-**1** (π-donor) with the π-acceptor molecules (*E*)-**2b,c** in MeCN in the concentration range up to 0.05 M for **1** and up to 1×10^{-3} M for the acceptor is perfectly described by the following equilibria:

$$\mathbf{D} + \mathbf{A} \overset{K_1}{\rightleftarrows} \mathbf{D \cdot A} \quad (1)$$

$$\mathbf{D \cdot A} + \mathbf{D} \overset{K_2}{\rightleftarrows} \mathbf{D \cdot A \cdot D} \quad (2)$$

where **D** is the donor, **A** is the acceptor, and K_1 (M^{-1}) and K_2 (M^{-1}) are the equilibrium constants. Spectrophotometric titration experiments on systems **1**/**3** and **1**/**4** (see Experimental Section) showed that this reaction model also holds true for acceptors **3** and **4** (Scheme 2).

Figures 1 and 2 show the CT absorption spectra of the **D**·**A** and **D**·**A**·**D** complexes involving acceptors **3b,c** and **4b,c**, respectively. The formation constants K_1 and K_2 and the main characteristics of the low-energy CT absorption band for the bi- and termolecular complexes are listed in Table 1.

In the region $\lambda > 400$ nm, where neither **1** nor **3b,c** absorb the light, complexes [**1**·**3b,c**] demonstrate a broad low-intensity absorption band, which is indicative of through-space CT interaction between the donor and the acceptor. In the case of [**1**·**4b,c**], the CT absorption reveals itself as a long-wavelength shoulder of the intense band associated with the local S_0-S_1 electronic transition of the acceptor moiety (the absorption spectra of diazapyrene derivatives **4b,c** are presented in Figure S28, Supporting Information).

The termolecular complexes [**1**·**3b,c**·**1**] and [**1**·**4b,c**·**1**] exhibit more intense CT absorption bands peaked at longer wavelengths as compared with the corresponding bimolecular complexes. With acceptors (*E*)-**2b,c**, transition from **D**·**A** to **D**·**A**·**D** also leads to a red shift of the CT absorption band,[9b] i.e., to a decrease in the energy of CT electronic transition (ΔE_{CT}). At least two factors can be responsible for this feature. First,

dx.doi.org/10.1021/jo201172w |*J. Org. Chem.* 2011, 76, 6768–6779

Scheme 2. Formation of CT Complexes D·A and D·A·D

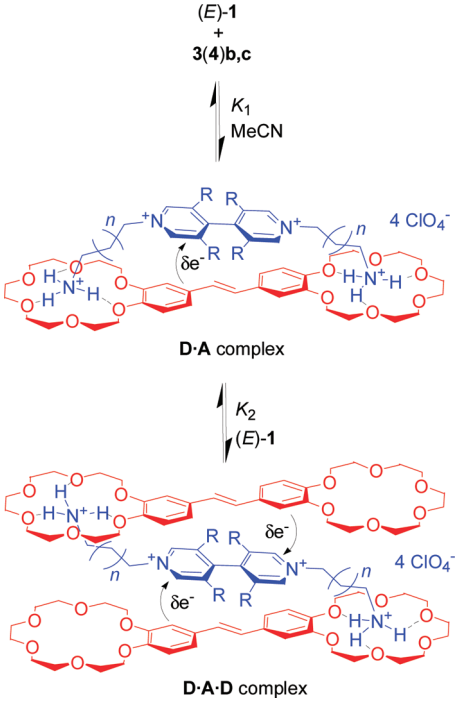

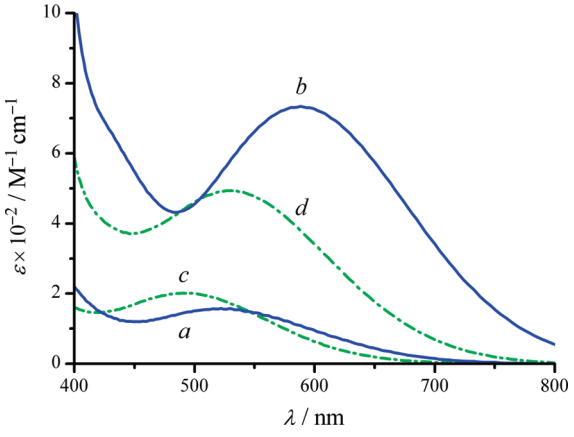

Figure 1. CT absorption spectra of (*a*) [**1·3b**], (*b*) [**1·3b·1**], (*c*) [**1·3c**], and (*d*) [**1·3c·1**] in MeCN.

ΔE_{CT} of symmetrical **D·A·D** complexes can be affected by coupling of two equivalent CT excited states.[10] Second, the termolecular complexes have less sterically strained structures than the pseudocyclic **D·A** systems, resulting in shorter donor−acceptor separation distance and, consequently, stronger CT interaction between the donor and the acceptor.

In the case of **3b**, the transition from **D·A** to **D·A·D** is accompanied by the most significant change of CT absorption: the low-energy CT band shifts bathochromically by 66 nm, and its intensity increases by a factor of 4.5. We suppose that the bipyridinium fragment in [**1·3b**] has a nonplanar geometry, typical of viologen derivatives. In [**1·3b·1**], this fragment is likely to adopt a more planar conformation due to stacking with the two stilbene fragments, which provides relatively large gain in the CT interaction.

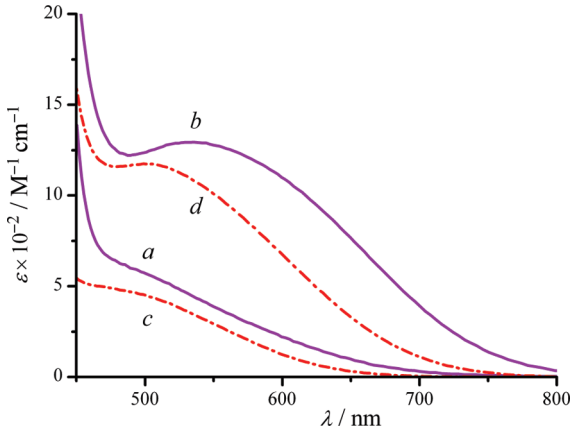

Figure 2. CT absorption spectra of (*a*) [**1·4b**], (*b*) [**1·4b·1**], (*c*) [**1·4c**], and (*d*) [**1·4c·1**] in MeCN.

Table 1. Formation Equilibrium Constants and Characteristics of the Low-Energy CT Absorption Band for the Bi- and Termolecular Complexes between (*E*)-1 and Compounds 2−4

	D·A			D·A·D		
acceptor (A)	log K_1[a]	λ_{max}, nm	ε_{max}, $M^{-1}\cdot cm^{-1}$	log K_2[a]	λ_{max}, nm	ε_{max}, $M^{-1}\cdot cm^{-1}$
2b[b]	9.42	535	340	2.73	555	900
2c[b]	9.08	502	390	3.20	519	1020
3b	7.36	522	160	2.73	588	730
3c	9.15	493	200	1.73	530	490
4b	7.72	*c*	*c*	3.30	535	1290
4c	9.39	*c*	*c*	2.33	503	1170

[a] MeCN, 23 ± 1 °C. K_1 = [**D·A**]/([**D**] × [**A**]) (M^{-1}), K_2 = [**D·A·D**]/([**D·A**] × [**D**]) (M^{-1}). The formation constants are measured to within ±20%. [b] From ref 9b. [c] Shoulder (see Figure 2).

The change from the ammoniopropyl to ammonioethyl tails in acceptors **2**−**4** results in a decrease in ΔE_{CT} for both bi- and termolecular complexes. This feature can be explained by a shorter donor−acceptor separation distance in the complexes having shorter ammonioalkyl spacers.

For common organic donor−acceptor complexes, ΔE_{CT} normally decreases with a decrease in the reduction potential of the acceptor. In the case of supramolecular **D·A** complexes, we observe some deviations from this correlation. For example, viologen derivative **3c** is a stronger electron acceptor than **2c** (see below); nevertheless, complex [**1·3c**] shows a higher ΔE_{CT} than [**1·2c**]. This fact suggests that complexes [**1·3c**] and [**1·2c**] significantly differ from each other in the reorganization energy associated with the photoinduced charge transfer reaction.[7]

Figure 3 shows the log K_1 and log K_2 values for the bi- and termolecular CT complexes as functions of the distance between the ammonium nitrogen atoms in the acceptor molecule (R_{am}). The R_{am} values were determined by quantum-chemical calculation of the geometry of **2**−**4** in MeCN. Acceptors **2**−**4** are divided into two groups. Group I comprises compounds in which the π-acceptor fragment has a planar geometry (**2b,c** and **4b,c**). Group II includes compounds with a nonplanar π-acceptor fragment (**3b,c**).

The dependences presented in Figure 3 have two specific features. First, in the region of R_{am} = 16.0−16.5 Å, the log K_1

dx.doi.org/10.1021/jo201172w |*J. Org. Chem.* 2011, 76, 6768–6779

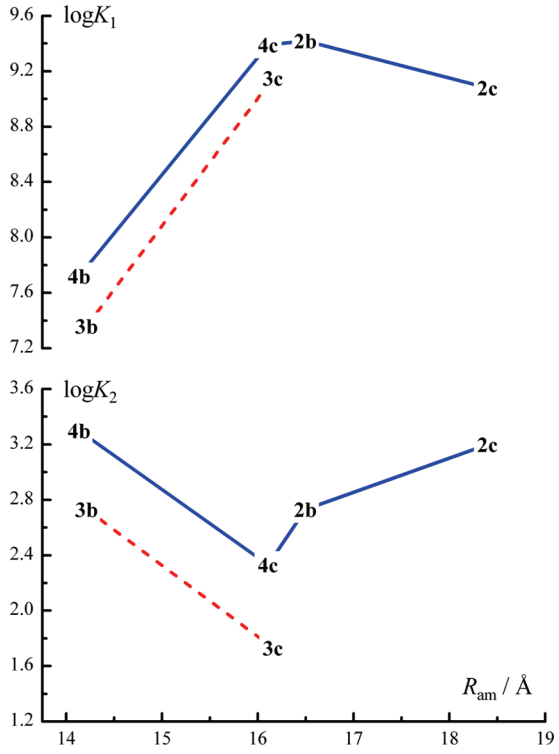

Figure 3. Formation equilibrium constants for the CT complexes **D·A** and **D·A·D** vs the distance between the ammonium nitrogen atoms in the acceptor molecule, R_{am}.

values for acceptors of both groups reach a maximum and the log K_2 values reach a minimum. Second, the plots of log K_1 vs R_{am} and log K_2 vs R_{am} for acceptors of group I lie above the corresponding plots for viologens **3b,c**. These two specific features can be interpreted using the general views on the driving force of formation of complexes **D·A** and **D·A·D**.[9b]

Undoubtedly, the main driving force of the formation of pseudocyclic bimolecular complexes is two-center hydrogen bonding. This bonding is most effective when there is exact geometric correspondence between the reactants. Any change in the geometry of one reactant (e.g., the change in the length of ammonioalkyl tails in **2**−**4**) would result in excess steric strain in the pseudocyclic complex **D·A**. For systems **1**/**2**−**4**, the best geometric correspondence for the two-center hydrogen bonding is attained apparently for R_{am} = 16.0−16.5 Å, where log K_1 for acceptors of both groups are maximum.

A certain contribution to the free energy of formation of complexes **D·A** can be made by stacking interactions between the unsaturated fragments of **D** and **A**. The acceptors having a planar unsaturated fragment (group I) are more prone to stacking interactions; therefore, the plot of log K_1 vs R_{am} for these acceptors runs above the corresponding plot for viologens **3b,c**.

A key driving force of the reaction **D·A** + **D** → **D·A·D** is the excessive steric strain in the pseudocyclic **D·A** structures, which is released upon transition to the **D·A·D** complexes. This conclusion is consistent with the fact that the positions of the minima in the log K_2 vs R_{am} plots coincide with the maxima in the log K_1 vs R_{am} plots (the maxima correspond to the **D·A** complexes having the lowest steric strain).

The three-decker structure of **D·A·D** complexes suggests stronger stacking interactions than those possible in pseudocyclic **D·A** precursors. This is another factor that can promote the reaction **D·A** + **D** → **D·A·D**. In the case of group I acceptors, this factor does make a significant contribution to the free energy of this reaction; this conclusion follows from a comparison of the two plots of log K_2 vs R_{am}.

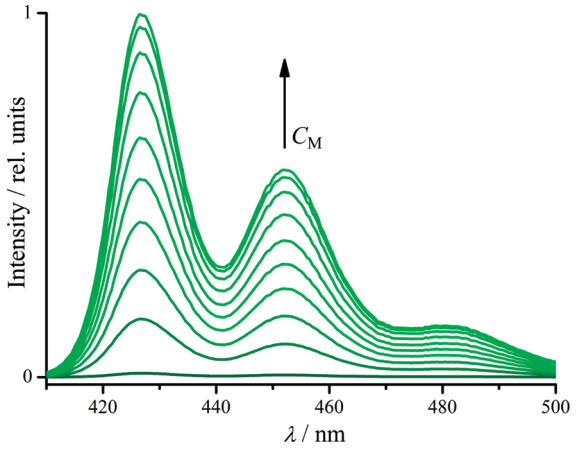

Figure 4. Fluorescence spectra in acetonitrile containing CT complex [**1·4c**] at a concentration of 1.0 × 10^{-5} M and $Ca(ClO_4)_2$ at different concentrations, C_M, ranging from 0 to ca. 7 × 10^{-5} M; excitation at 402 nm. The spectra are assigned to the uncomplexed diazapyrene derivative **4c**.

Fluorescence Studies. CT complex [**1·4c**] was tested for use as a fluorescent sensor for alkaline-earth metal ions. Figure 4 shows the fluorescence spectra in acetonitrile containing [**1·4c**] at a concentration, $C_{D·A}$, of 1.0 × 10^{-5} M and $Ca(ClO_4)_2$ at different concentrations, C_M, ranging from 0 to ca. 7 × 10^{-5} M (excitation at 402 nm).

Complex [**1·4c**] is intrinsically nonfluorescent, but its solution shows a very weak fluorescence coming from the uncomplexed **4c** molecules, the percentage of which at $C_{D·A}$ = 1.0 × 10^{-5} M is <1%. On addition of $Ca(ClO_4)_2$, the percentage of uncomplexed **4c** molecules increases due to the binding of Ca^{2+} ions to the crown-ether fragments of stilbene **1** (Scheme 3), which results in an increase in the fluorescence intensity (the fluorescence quantum yield of **4c** in MeCN was estimated to be 0.31).

Figure 5 shows the dependencies of fluorescence yield (Φ_f) on the concentration of metal perchlorate for acetonitrile solutions of [**1·4c**]/$Mg(ClO_4)_2$, [**1·4c**]/$Ca(ClO_4)_2$, and [**1·4c**]/$Ba(ClO_4)_2$ ($C_{D·A}$ = 1.0 × 10^{-5} M, excitation at 402 nm). These data demonstrate a high selectivity of the fluorescence response of complex [**1·4c**] toward Ca^{2+} and Ba^{2+} versus Mg^{2+}.

The molar absorptivities of complex [**1·4c**] and compound **4c** at 402 nm are equal (see Figure S37, Supporting Information); therefore, the fluorescence yield Φ_f is directly proportional to the concentration of uncomplexed **4c** molecules (note that bis(crown)stilbene **1** and its complexes with alkaline-earth metal ions do not absorb the light with λ > 400 nm). The dependencies of Φ_f on $C_M/C_{D·A}$ measured for $Ca(ClO_4)_2$ and $Ba(ClO_4)_2$ were interpreted in terms of the complexation model comprising the equilibria of eqs 1 and 3:

$$\mathbf{D} + 2M^{2+} \overset{K_M}{\rightleftarrows} \mathbf{D}\cdot(M^{2+})_2 \qquad (3)$$

where M is the metal cation and K_M is the complex stability constant. The best fits to this model (Figure 5) were found when log K_M = 15.5 for Ca^{2+} and 16.5 for Ba^{2+}.

dx.doi.org/10.1021/jo201172w |J. Org. Chem. 2011, 76, 6768–6779

Scheme 3. Reaction of Ca^{2+} with Complex [1·4c]

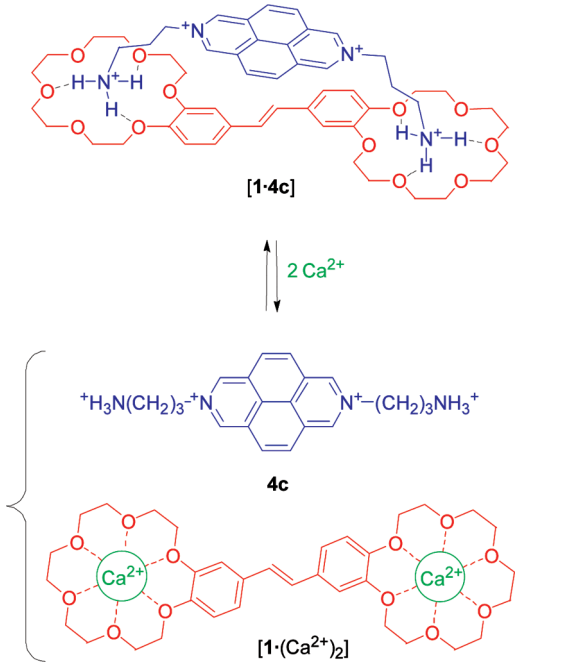

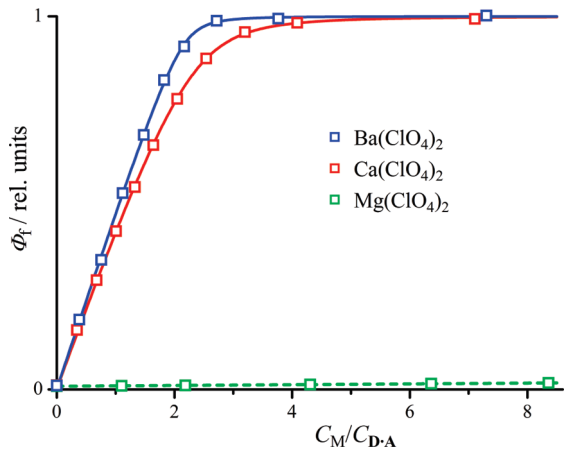

Figure 5. Fluorescence yield, Φ_f, as a function of the concentration of metal perchlorate for acetonitrile solutions of [**1·4c**]/$Mg(ClO_4)_2$, [**1·4c**]/$Ca(ClO_4)_2$, and [**1·4c**]/$Ba(ClO_4)_2$ ($C_{D\cdot A} = 1.0 \times 10^{-5}$ M, excitation at 402 nm). The solid curves are the best fits to the complexation model comprising the equilibria of eqs 1 and 3.

Redox Properties. The electrochemical properties of the supramolecular CT complexes [**1·3b,c**] and [**1·4b,c**] were studied using cyclic voltammetry at a glassy carbon electrode in acetonitrile containing Bu_4NClO_4 (0.1 M). Selected cyclic voltammograms are shown in Figure S39 (Supporting Information). The peak potentials of the first redox transitions, vs Ag|AgCl|KCl (aq., sat.), for complexes [**1·2b,c**], [**1·3b,c**], and [**1·4b,c**] as well as for the uncomplexed compounds **1**, **2b,c**, **3b,c**, and **4b,c** are presented in Table 2. The electrochemical data for systems **1**/**2b,c** are taken from ref 11.

The formation of pseudocyclic **D·A** complexes is accompanied in all cases by a considerable anodic shift of the first oxidation potential of donor **1**, and the first redox transition becomes irreversible. The anodic shift ΔE_p^{ox} varies from 130 to 240 mV depending on the acceptor structure. The more difficult oxidation of complexed **1** compared with free **1** is caused by two factors. First, the two-center interaction of the ammonium groups of the acceptor with the heteroatoms of the crown-ether fragments of **1** through hydrogen bonding reduces the electron density on the π-electron-donor fragment of **1**. In sterically strained [**1·3b**] and [**1·4b**], this interaction is least effective; hence, [**1·3b**] and [**1·4b**] have the lowest ΔE_p^{ox} values. Second, the oxidized form of **1**, i.e., the radical cation $\mathbf{1}^{\bullet+}$, in the complex with the tetracationic acceptor is destabilized due to Coulomb repulsion.

The first reduction potentials of the complexes **D·A** are shifted to less negative values relative to the reduction potential of the free acceptor. The magnitude of this shift, ΔE_p^{red}, varies in the range of 10−100 mV depending on the acceptor structure. In all cases except for **4b**, the redox transition remains reversible. A positive value of ΔE_p^{red} implies that the reduced form of the acceptor is more stable when complexed with **1** than in the free state. Note that for complexes **D·A**, the positive shift of the reduction potential of the acceptor is consistent with the decrease in the energy of the local S_0-S_1 electronic transition of the acceptor (see Figures S31 and S32 for **4b,c** (Supporting Information)).

Electrochemical data for various supramolecular viologen complexes have been reported, in particular, "host−guest" complexes with cyclodextrins,[12] calixarenes,[13] cucurbiturils,[14] aromatic molecular pincers,[15] and pseudorotaxane donor−acceptor complexes.[16] In most cases, the complexation induced a negative shift of the first reduction potential of viologen. The exceptions are the inclusion complexes with β- and γ-cyclodextrins and cucurbit[8]uril, for which an opposite effect is observed. The positive shift of the reduction potential in the methylviologen/β-cyclodextrin system[12a] is because of the fact that β-cyclodextrin does not bind methylviologen but can encapsulate its reduced form. In the case of complexes formed by viologens with γ-cyclodextrin[12a] and cucurbit[8]uril,[14b] the positive shift of the reduction potential is caused by stabilization of the viologen radical cation dimer in the host cavity.

It is evident that these mechanisms are inappropriate for interpreting the positive ΔE_p^{red} values observed for pseudocyclic complexes [**1·2b,c**], [**1·3b,c**], and [**1·4b,c**]. Presumably, easier reduction of the complexed acceptor as compared with its free molecule is attributable, first, to considerable changes in the solvation shell of the charged acceptor molecule upon the formation of the pseudocyclic complex, and second, to specific interaction of the reduced form of the acceptor with the stilbene fragment of **1**.

^{1}H NMR Spectroscopy Studies. The addition of equimolar amounts of compounds **3b,c** or **4b,c** to MeCN-d_3 solutions of (*E*)-**1** induced considerable shifts of most proton signals, $\Delta\delta_H$, in the ^{1}H NMR spectra (e.g., Figure 6a−c), indicating the formation of pseudocyclic **D·A** complexes in which the components are arranged one above another (Scheme 2). The $\Delta\delta_H$ values measured for these equimolar mixtures are shown in Figure 7. The downfield shifts of most CH_2O signals ($\Delta\delta_H$ of up to 0.24 ppm) are attributable to the electron-withdrawing effect of the ammonium ions bound to the crown-ether fragments of **1**. Most of the proton signals corresponding to the central fragments of the donor and the acceptor show upfield shifts due to the mutual shielding effect ($\Delta\delta_H$ of up to −1.17 ppm).

As the content of **1** in solution increases, the proton signals of the acceptor continue to regularly shift upfield (see Figure 6c,d).

dx.doi.org/10.1021/jo201172w |*J. Org. Chem.* 2011, 76, 6768–6779

Table 2. Peak Potentials of the First Redox Transitions for π-Electron Donor (*E*)-1, π-Electron Acceptors 2−4, and Supramolecular D·A Complexes[a]

compound	E_p^{ox}/E_p^{red}/V	complex	E_p^{ox}/V	E_p^{red}/V	ΔE_p^{ox}/mV[b]	ΔE_p^{red}/mV[b]
1[c]	1.0 rev/−2.48					
2b[c]	−/−0.50 rev	[**1**·**2b**][c]	1.24	−0.43 rev	240	70
2c[c]	−/−0.50 rev	[**1**·**2c**][c]	1.24	−0.43 rev	240	70
3b	−/−0.40 rev	[**1**·**3b**]	1.13	−0.33 rev	130	70
3c	−/−0.41 rev	[**1**·**3c**]	1.19	−0.38 rev	190	30
4b	−/−0.42 rev	[**1**·**4b**]	1.15	−0.32	150	100
4c	−/−0.43 rev	[**1**·**4c**]	1.20	−0.42 rev	200	10

[a] MeCN, supporting electrolyte Bu_4NClO_4 (0.1 M), glassy carbon electrode vs Ag|AgCl|KCl (aq., sat.), rev denotes reversible (the forward to reverse peak potential difference is about 60 mV). [b] $\Delta E_p^{ox} = E_p^{ox}$(complex) − E_p^{ox}(free donor). $\Delta E_p^{red} = E_p^{red}$(complex) − E_p^{red}(free acceptor). [c] From ref 11.

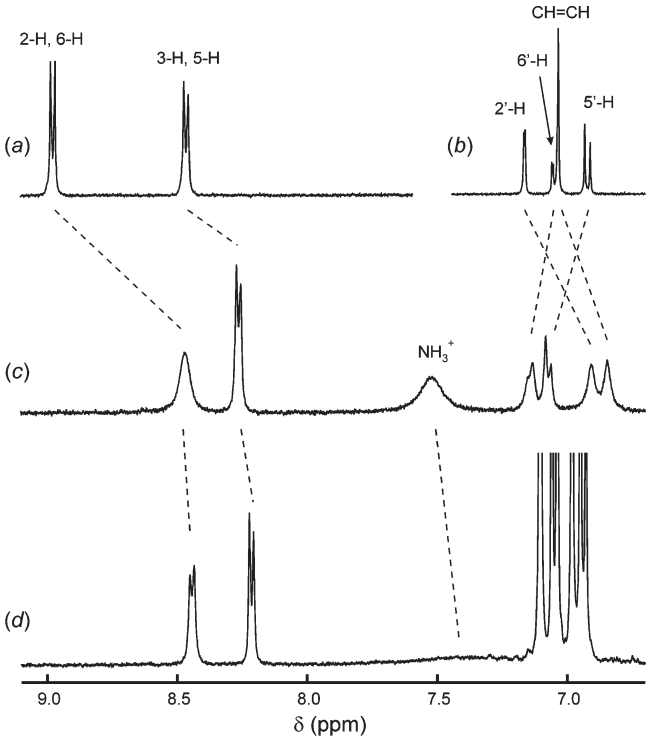

Figure 6. ^{1}H NMR spectra (aromatic proton region) of (*a*) **3c** (1×10^{-3} M), (*b*) (*E*)-**1** (1×10^{-3} M), and their mixtures in molar ratios (*c*) 1:1 and (*d*) 1:6 (500.13 MHz, MeCN-d_3, 25 °C).

This implies transition from the bimolecular **D**·**A** complex to termolecular **D**·**A**·**D** complex, in which the acceptor molecule is sandwiched between two bis(crown)stilbene molecules (Scheme 2), and, hence, the acceptor hydrogen atoms become even more shielded.

Detailed analysis of the $\Delta\delta_H$ values presented in Figure 7 shows that the unsaturated fragments of the donor and acceptor molecules in the **D**·**A** complexes are not located exactly one above another but are preferably projected X-wise. It is this arrangement of the unsaturated fragments that occurs for complexes [**1**·**3c**] in the crystal (see below). Figure 8 shows schematically the intermolecular NOE interactions found for systems [**1**·**3b**,**c**]. All of the detected intermolecular NOE cross peaks are weak as compared with intramolecular NOE signals; therefore, the distances between the interacting protons can be roughly estimated as ranging from 3.0 to 3.5 Å. The number of intermolecular NOE interactions increases with a decrease in the linear dimensions of the diammonium compound, evidently, due to a decrease in the donor−acceptor separation distance.

The complex formation constants for systems **1**/**2**(**3**,**4**)**a**−**c** were estimated using ^{1}H NMR titration (see Experimental Section). For model acceptors **3a** and **4a**, the experimental dependences of $\Delta\delta_H$ on the amount of **1** added were interpreted in terms of 1:1 complex formation. For diammonium compounds **2**(**3**,**4**)**b**,**c**, the ^{1}H NMR titration data were described well by the complexation model comprising the equilibria of eqs 1 and 2. The measured log K_1 and log K_2 values are presented in Table 3.

Good agreement between the log K_2 values determined by NMR spectroscopy and spectrophotometry (compare the data in Tables 3 and 1) confirms the applicability of the approaches used. For the supramolecular **D**·**A** complexes, the log K_1 values derived from ^{1}H NMR experiments are lower by 0.1−0.6 than those measured by spectrophotometry. This is attributable to a higher content of water impurity in MeCN-d_3. The presence of water can lead to a decrease in the equilibrium constant K_1 of eq 1 due to preferable hydration of uncomplexed ammonium ions (this factor has less influence on the equilibrium of eq 2).

For the model acceptors, the complex stability constants K_1 are relatively low (log K_1 < 1.7) and increase in the series **3a** < **2a** < **4a**, which evidently reflects the enhancement of the stacking interactions in the complexes following increase in the conjugation system of the acceptor. The huge differences in the K_1 values between the model acceptors and the corresponding diammonium compounds (**2**−**4**)**b**,**c** clearly attest that the two-center hydrogen bonding in the supramolecular **D**·**A** complexes makes a much greater contribution to the free energy of complex formation than the stacking interactions between the unsaturated fragments of the components.

X-ray Diffraction Studies. Compounds **3c** and **4a** and complexes [**1**·**3b**] and [**1**·**3c**] were grown as single crystals suitable for X-ray diffraction analysis. The structures of the key crystal components are shown in Figure 9.

In the structure of **3c**·$2H_2O$, the viologen tetracation is located at the symmetry center of the crystal, which coincides with the midpoint of the C(6)−C(6A) bond connecting two pyridine residues. Because of this position, the bipyridinium fragment occurs in an ideally planar conformation. Note that X-ray diffraction study of the model viologen **3a** has shown[9a] that its pyridinium rings are twisted by 15.8°; this is more typical of 4,4′-bipyridine derivatives due to the steric interaction of the *ortho*-hydrogen atoms.

The distance between the N(1) and N(1A) atoms of ammonium groups in **3c** is 16.13 Å, which practically coincides with the calculated data. The $N(1)H_3^+$ group forms a network of

dx.doi.org/10.1021/jo201172w |*J. Org. Chem.* 2011, 76, 6768–6779

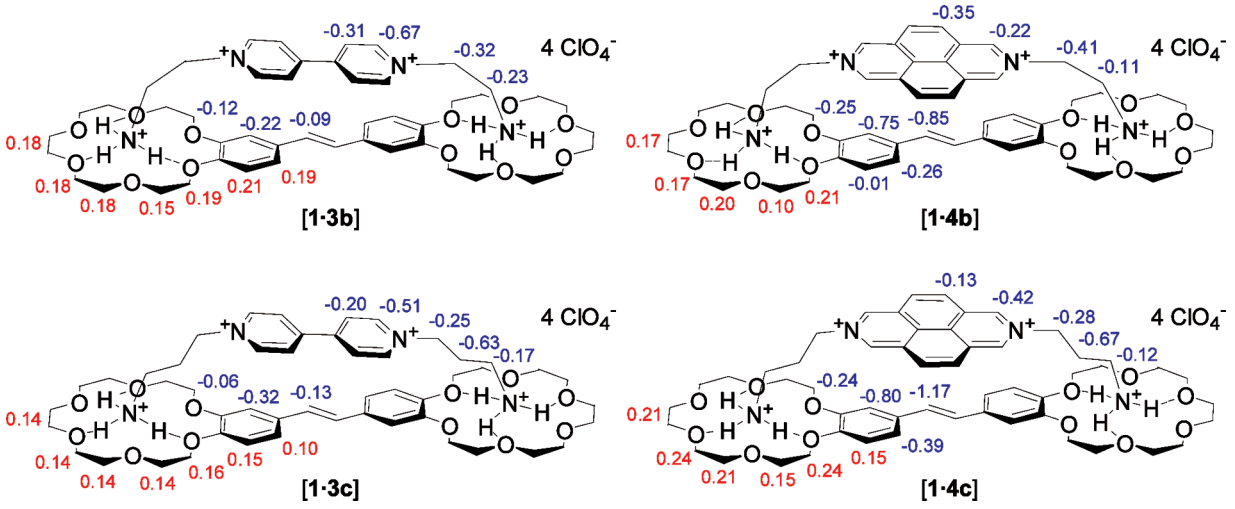

Figure 7. Changes in the proton chemical shifts, $\Delta\delta_H = \delta_H(\text{complex}) - \delta_H(\text{free compound})$, upon complexation of (*E*)-**1** with **3b**,**c**, **4b**,**c** (500.13 MHz, MeCN-d_3, 25 °C) (red = deshielding, blue = shielding).

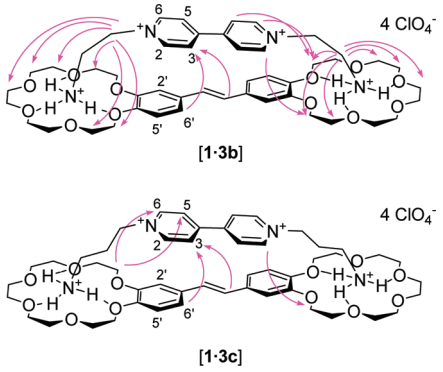

Figure 8. Intermolecular NOE interactions detected for complexes [**1**·**3b**] and [**1**·**3c**].

Table 3. Formation Equilibrium Constants for the Bi- and Termolecular Complexes between (*E*)-1 and Compounds 2−4, as Derived from ^{1}H NMR Titration Experiments[a]

acceptor	log K_1	log K_2
2a	1.14[b]	
2b	9.0	2.78[b]
2c	8.9	3.27[b]
3a	0.86	
3b	6.8	2.72
3c	8.9	1.79
4a	1.65	
4b	7.1	3.22
4c	9.3	2.34

[a] MeCN-d_3, 25 ± 1 °C. K_1 = [**D**·**A**]/([**D**] × [**A**]) (M^{-1}), K_2 = [**D**·**A**·**D**]/([**D**·**A**] × [**D**]) (M^{-1}). The formation constants are measured to within ±20%. [b] From ref 9b.

hydrogen bonds with the oxygen atoms of two independent perchlorate anions and with the O(1W) water molecule.

In the structure of model compound **4a**, the diazapyrene dication is located at the symmetry center of the crystal, which determines the perfectly planar conformation of its conjugated fragment. Note that the planarity of the diazapyrene fragment is rather predetermined by its rigid structure, although upon stacking, this fragment can be noticeably crooked, as shown in our study[9a] of the crystal structure of the benzene solvate of **4a**.

It has been shown previously[9b] that crystalline free stilbene (*E*)-**1** is the s-*anti*,s-*anti*-conformer. In solutions, (*E*)-**1** exists as an equilibrated mixture of s-*anti*,s-*anti*- and s-*syn*,s-*syn*-conformers (Scheme 4); according to ^{1}H NMR data, more compact s-*syn*,s-*syn*-conformer predominates.[8] In crystalline complexes [**1**·**3b**] and [**1**·**3c**], stilbene **1** is revealed as an s-*syn*,s-*syn*-conformer (Figure 9c,d).

The structure [**1**·**3c**]·0.25MeCN·0.44H_2O contains two independent pseudocyclic complexes [**1**·**3c**], differing by the conformations of the donor and acceptor components. In one complex, two $(CH_2)_3NH_3^+$ groups occur in different conformations (*trans*,*trans* and *trans*,*gauche*). In the other independent complex, both $(CH_2)_3NH_3^+$ groups have a fully transoid conformation. In pseudocyclic complexes, the ammonium groups are located on one side of the mean plane of the bipyridinium fragment; therefore, the distances between the ammonium nitrogen atoms, N(1)···N(4) (14.71 Å) and N(1′)···N(4′) (14.23 Å), are smaller than this parameter in **3c**·2H_2O. Each ammonium group forms directed hydrogen bonds with three oxygen atoms of the 18-membered macrocycle; the N···O(macrocycle) distances are in the range of 2.801(6)−2.940(6) Å.

Note that the bipyridinium fragments in both independent complexes [**1**·**3c**] are nonplanar: the dihedral angles between the pyridinium rings, N(2)C_5/N(3)C_5 and N(2′)C_5/N(3′)C_5, are 34.2 and 35.9°, respectively. The stilbene fragments in these complexes also have nonplanar conformations: the dihedral angles between the benzene rings, C(11), ..., C(16)/C(28), ..., C(33) and C(11′), ..., C(16′)/C(28′), ..., C(33′), are 24.8 and 31.1°, respectively. These facts imply relatively weak stacking interactions in crystalline complexes [**1**·**3c**].

In [**1**·**3b**]·$C_4H_8O_2$·3H_2O, both the stilbene fragment of **1** and the bipyridinium fragment of **3b** have a perfectly planar structure because the midpoints of the C(17)═C(17A) and C(5′)−C(5′A) bonds coincide with the symmetry centers of the crystal. However, in this case, a different crystal packing motif is observed. The centrosymmetric structure of tetracation **3b** implies that the ammonioethyl N-substituents are located on

dx.doi.org/10.1021/jo201172w |*J. Org. Chem.* 2011, 76, 6768–6779

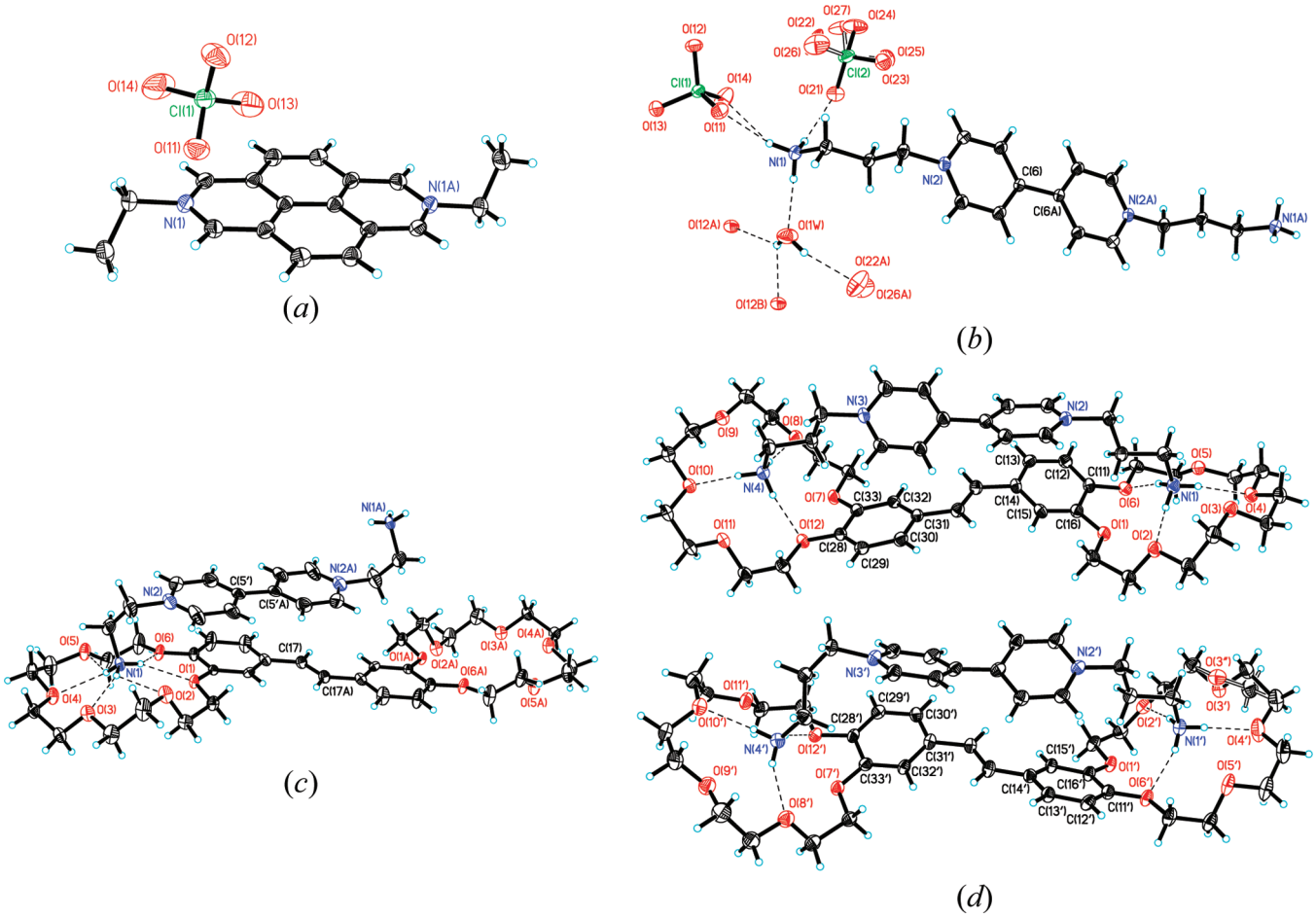

Figure 9. Structures of the main components of the crystals (*a*) **4a**, (*b*) **3c**·2H_2O, (*c*) [**1**·**3b**]·$C_4H_8O_2$·3H_2O, and (*d*) [**1**·**3c**]·0.25MeCN·0.44H_2O (two independent complexes). Thermal anisotropic ellipsoids are drawn at the (*a*, *b*) 50, (*c*) 40, and (*d*) 30% probability level. The additional letters "A" and "B" indicate that atoms belong to symmetrically related positions. Hydrogen bonds are drawn with dash lines.

Scheme 4. Conformers of (*E*)-1

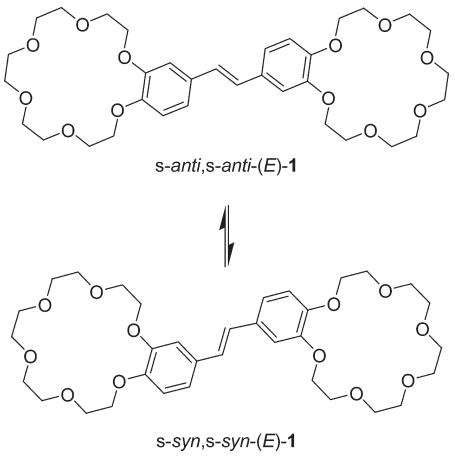

different sides of the plane of bipyridinium fragment (the distance between the N(1) and N(1A) atoms is 11.68 Å). This gives rise to infinite skewed $(\mathbf{D}\cdot\mathbf{A})_m$ type stacks consisting of alternating donor and acceptor molecules hydrogen-bonded to one another (Figure 10). The ammonium groups of **3b** mainly form bifurcate hydrogen bonds with the oxygen atoms of 18-membered macrocycles. Here the N···O(macrocycle) distances are in the range of 2.839(9)−2.969(9) Å. Thus, owing to the formation of the coordination polymer, the relatively short viologen **3b** molecule and the bis(18-crown-6)stilbene molecule can avoid considerable twisting of their central fragments, which would inevitably arise upon the formation of pseudocyclic complexes as is the case for complex [**1**·**3c**]. In structure [**1**·**3b**], the dihedral angle between the mean planes of the stilbene and bipyridinium fragments adjoining each other in the stack is only 4.5° and the interplanar spacing is 3.4 Å. This structure allows relatively strong stacking interactions in the crystalline state without considerable steric strain.

CONCLUSIONS

4,4′-Bipyridine **3b**,**c** and 2,7-diazapyrene **4b**,**c** derivatives (acceptors, **A**) containing two ammonioalkyl N-substituents interact with bis(18-crown-6)stilbene **1** (donor, **D**) to form supramolecular 1:1 (**D**·**A**) and 2:1 (**D**·**A**·**D**) CT complexes. CT complex [**1**·**4c**] in nonaqueous media performs as a fluorescent sensor with a very selective response toward Ca^{2+} and Ba^{2+} versus Mg^{2+}. The key driving force of the formation of pseudocyclic **D**·**A** complexes is the macrocycle−ammonium cation ditopic binding; therefore, the better the geometric matching between the components for the ditopic binding, the

dx.doi.org/10.1021/jo201172w |*J. Org. Chem.* 2011, 76, 6768–6779

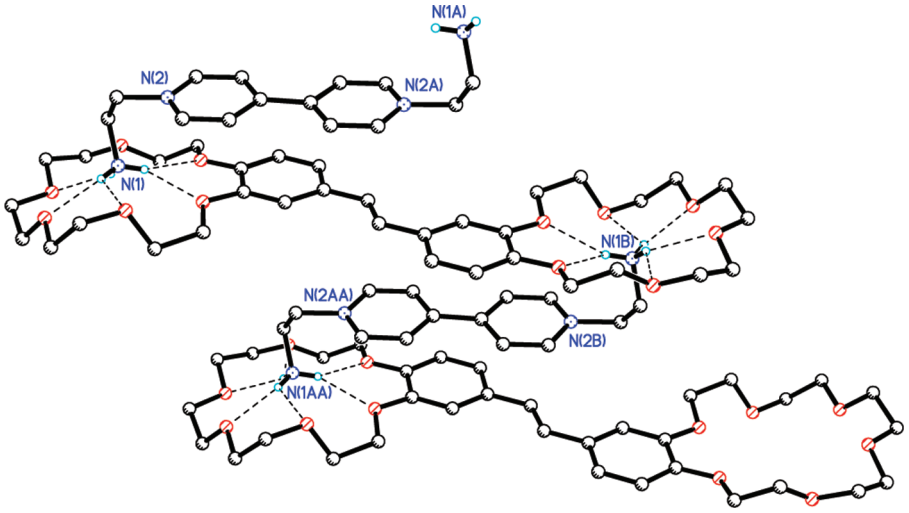

Figure 10. Stacking of $(\mathbf{D}\cdot\mathbf{A})_m$ type in structure $[\mathbf{1}\cdot\mathbf{3b}]\cdot C_4H_8O_2\cdot 3H_2O$. Most of the hydrogen atoms, perchlorate anions, and solvate molecules are omitted for clarity. Hydrogen bonds are drawn with dash lines.

higher the stability of the **D·A** complexes. A key driving force of the **D·A** + **D** → **D·A·D** reaction resulting in unusual three-decker CT complexes is the steric strain in the pseudocyclic **D·A** complexes. Yet another factor promoting this reaction is the ability of the π-acceptor and π-donor fragments to undergo stacking interactions. The transition from **D·A** to **D·A·D** can be accompanied by considerable enhancement of stacking interactions as the steric strain is rather low in the three-decker **D·A·D** structures. Analogous causes induce the transition of the **D·A** complexes to structures like the $(\mathbf{D}\cdot\mathbf{A})_m$ coordination polymer upon crystallization. The found features of the construction of stacked **D·A** complexes can be used to design light-sensitive architectures in bottom-up nanotechnology.

EXPERIMENTAL SECTION

General Methods. The ^{1}H and ^{13}C NMR spectra were recorded in MeCN-d_3 and DMSO-d_6 using the solvent as the internal reference (δ_H 1.96 and 2.50, respectively; δ_C 39.4 for DMSO-d_6). 2D NOESY and HSQC spectra were used to assign the proton and carbon signals; the mixing time in the NOESY experiment was 300 μs.

Synthesis and characterization of bis(crown)stilbene (*E*)-**1** and acceptor compounds **2a,c** were described earlier.[6a,8]

*4,4′-(E)-Ethene-1,2-diylbis[1-(2-ammonioethyl)pyridinium] Tetraperchlorate (**2b**).* Compound **2b** was synthesized by a known method:[9b] mp 281−283 °C (decomp.); ^{1}H NMR (500.13 MHz, MeCN-d_3−$CDCl_3$ (24:1, v/v), 25 °C) δ 3.60 (t, J = 6.6 Hz, 4H, 2 CH_2NH_3), 4.84 (t, J = 6.6 Hz, 4H, 2 CH_2N), 7.94 (s, 2H, CH=CH), 8.31 (d, J = 6.9 Hz, 4H, 2 3-H, 2 5-H), 8.80 (d, J = 6.9 Hz, 4H, 2 2-H, 2 6-H) ppm; ^{13}C NMR (125.76 MHz, DMSO-d_6, 26 °C) δ 38.9 (2 CH_2NH_3), 57.7 (2 CH_2N), 125.5 (2 3-C, 2 5-C), 134.2 (CH=CH), 145.8 (2 2-C, 2 6-C), 150.9 (2 4-C) ppm.

*1,1′-Diethyl-4,4′-bipyridinium Diperchlorate (**3a**).* Compound **3a** was synthesized by a known method:[9a] mp 270−272 °C (decomp.); ^{1}H NMR (500.13 MHz, MeCN-d_3, 25 °C) δ 1.68 (t, J = 7.3 Hz, 6H, 2 Me), 4.70 (q, J = 7.3 Hz, 4H, 2 CH_2), 8.40 (m, 4H, 2 3-H, 2 5-H), 8.94 (d, J = 6.8 Hz, 4H, 2 2-H, 2 6-H) ppm; ^{13}C NMR (125.76 MHz, DMSO-d_6, 25 °C) δ 16.2 (2 Me), 56.5 (2 CH_2N), 126.5 (2 3-C, 2 5-C), 145.5 (2 2-C, 2 6-C), 148.5 (2 4-C) ppm.

*2,7-Diethylbenzo[lmn]-3,8-phenanthrolinediium Diperchlorate (**4a**).* Compound **4a** was synthesized by a known method:[9a] mp 322 °C (decomp.); ^{1}H NMR (500.13 MHz, MeCN-d_3, 25 °C) δ 1.90 (t, J = 7.3 Hz, 6H, 2 Me), 5.16 (q, J = 7.3 Hz, 4H, 2 CH_2), 8.85 (s, 4H, 4-H, 5-H, 9-H, 10-H), 9.92 (s, 4H, 2 1-H, 3-H, 6-H, 8-H) ppm; ^{13}C NMR (125.76 MHz, DMSO-d_6, 26 °C) δ 16.5 (2 Me), 58.5 (2 CH_2N), 126.0 (10b-C, 10c-C), 128.7 (3a-C, 5a-C, 8a-C, 10a-C), 129.7 (4-C, 5-C, 9-C, 10-C), 141.6 (1-C, 3-C, 6-C, 8-C) ppm.

Synthesis of *N,N′*-Di(ammonioalkyl) Derivatives 3b,c and 4b,c (General Method). A mixture of 4,4′-bipyridine or 2,7-diazapyrene[17] (1 mmol) and 2-bromoethylammonium bromide or 3-bromopropylammonium bromide (6 mmol) in dry MeCN (20 mL) was refluxed with stirring for 140 h. The reaction mixture was cooled to room temperature, and a precipitate that formed was filtered, washed with abs. EtOH (4 × 20 mL) and chloroform (2 × 10 mL), and dissolved in water (20 mL). The aqueous solution was filtered and evaporated in vacuo to give the tetrabromide salt of corresponding *N,N′*-di(ammonioalkyl) derivative as a yellow solid. The tetrabromide salt was dissolved upon heating in a mixture of EtOH (5 mL) and minimum quantity of water (several drops), and 70% aq. $HClO_4$ (0.6 mL, 7 mmol) and EtOH (5 mL) were added to the solution. The resulting solution was cooled to 5 °C, and a precipitate that formed was filtered, washed with EtOH (2 × 5 mL), and dried in air. This treatment was repeated using 70% aq. $HClO_4$ (0.3 mL, 3.5 mmol) to give the corresponding tetraperchlorate salt.

*1,1′-Bis(2-ammonioethyl)-4,4′-bipyridinium Tetraperchlorate (**3b**).* A white powder (0.18 g, 26% yield): mp 272−276 °C (decomp.); ^{1}H NMR (500.13 MHz, MeCN-d_3, 25 °C) δ 3.67 (t, J = 6.4 Hz, 4H, 2 CH_2NH_3), 4.94 (t, J = 6.4 Hz, 4H, 2 CH_2N), 8.53 (d, J = 6.8 Hz, 4H, 2 3-H, 2 5-H), 8.99 (d, J = 6.8 Hz, 4H, 2 2-H, 2 6-H) ppm; ^{13}C NMR (125.76 MHz, DMSO-d_6, 25 °C) δ 38.9 (2 CH_2NH_3), 58.1 (2 CH_2N), 126.4 (2 3-C, 2 5-C), 146.8 (2 2-C, 2 6-C), 148.8 (2 4-C) ppm; IR (Nujol) 3246, 3200 (N^+−H) cm^{-1}. Anal. Calcd. for $C_{14}H_{22}Cl_4N_4O_{16}\cdot 2H_2O$: C 24.72, H 3.85, N 8.24. Found: C 24.61, H 3.40, N 8.26.

*1,1′-Bis(3-ammoniopropyl)-4,4′-bipyridinium Tetraperchlorate (**3c**).* A white powder (0.48 g, 71% yield): mp 278−283 °C (decomp.); ^{1}H NMR (500.13 MHz, MeCN-d_3, 25 °C) δ 2.41 (m, 4H, 2 CH_2CH_2N), 3.13 (m, 4H, 2 CH_2NH_3), 4.72 (t, J = 7.7 Hz, 4H, 2 CH_2N), 8.47 (d, J = 6.7 Hz, 4H, 2 3-H, 2 5-H), 8.97 (d, J = 6.7 Hz, 4H, 2 2-H, 2 6-H) ppm; ^{13}C NMR (125.76 MHz, DMSO-d_6, 25 °C) δ 28.6 (2 CH_2CH_2N), 35.7 (2 CH_2NH_3), 58.0 (2 CH_2N), 126.6 (2 3-C, 2 5-C), 145.9 (2 2-C, 2 6-C), 148.8 (2 4-C) ppm; IR (Nujol) 3253, 3177 (N^+−H) cm^{-1}. Anal. Calcd. for $C_{16}H_{26}Cl_4N_4O_{16}\cdot 0.5H_2O$: C 28.21, H 4.00, N 8.23. Found: C 28.25, H 3.96, N 8.18.

dx.doi.org/10.1021/jo201172w |*J. Org. Chem.* 2011, 76, 6768–6779

*2,7-Bis(2-ammonioethyl)benzo[lmn][3,8]phenanthrolinediium Tetraperchlorate (**4b**).* A yellow powder (0.22 g, 32% yield): mp 335−338 °C (decomp.); ^{1}H NMR (500.13 MHz, MeCN-d_3, 30 °C) δ 3.91 (t, J = 6.2 Hz, 4H, 2 CH_2NH$_3$), 5.41 (t, J = 6.2 Hz, 4H, 2 CH$_2$N), 8.95 (s, 4H, 4-H, 5-H, 9-H, 10-H), 9.98 (s, 4H, 1-H, 3-H, 6-H, 8-H) ppm; ^{13}C NMR (125.76 MHz, DMSO-d_6, 25 °C) δ 39.4 (2 CH$_2$NH$_3$), 60.0 (2 CH$_2$N), 126.0 (10b-C, 10c-C), 128.8 (3a-C, 5a-C, 8a-C, 10a-C), 130.1 (4-C, 5-C, 9-C, 10-C), 142.8 (1-C, 3-C, 6-C, 8-C) ppm; IR (Nujol) 3172 (N$^+$−H) cm^{-1}. Anal. Calcd. for $C_{18}H_{22}Cl_4N_4O_{16}$: C 31.23, H 3.20, N 8.09. Found: C 31.17, H 3.21, N 8.11.

*2,7-Bis(3-ammoniopropyl)benzo[lmn][3,8]phenanthrolinediium Tetraperchlorate (**4c**).* A yellow powder (0.42 g, 58% yield): mp >340 °C (decomp.); ^{1}H NMR (500.13 MHz, MeCN-d_3, 30 °C) δ 2.66 (m, 4H, 2 CH_2CH$_2$N), 3.25 (br.m, 4H, 2 CH_2NH$_3$), 5.19 (t, J = 7.6 Hz, 4H, 2 CH$_2$N), 8.91 (s, 4H, 4-H, 5-H, 9-H, 10-H), 9.96 (s, 4H, 1-H, 3-H, 6-H, 8-H) ppm; ^{13}C NMR (125.76 MHz, DMSO-d_6, 25 °C) δ 28.9 (2 CH$_2$CH$_2$N), 35.8 (2 CH$_2$NH$_3$), 60.0 (2 CH$_2$N), 126.0 (10b-C, 10c-C), 128.9 (3a-C, 5a-C, 8a-C, 10a-C), 129.9 (4-C, 5-C, 9-C, 10-C), 142.0 (1-C, 3-C, 6-C, 8-C) ppm; IR (Nujol) 3192 (N$^+$−H) cm^{-1}. Anal. Calcd. for $C_{20}H_{26}Cl_4N_4O_{16}$: C 33.35, H 3.64, N 7.78. Found: C 33.39, H 3.58, N 7.74.

Synthesis of D·A Complexes between Stilbene 1 and Diammonium Compounds 3(4)b,c (General Method). Stilbene (*E*)-**1** (13 mg, 20 μmol) and a diammonium compound **3**(**4**)**b,c** (20 μmol) were dissolved in MeCN (5 mL). The solution was slowly saturated with a mixture of benzene and dioxane (~2:1, v/v) by a vapor diffusion method at ambient temperature until complete precipitation was attained (visual monitoring, 1−2 weeks). The crystalline precipitate was decanted and recrystallized in the same conditions to give supramolecular **D·A** complex as a fine-grained powder (amorphous powder in the case of [**1·3b**]). The complex stoichiometry was confirmed by ^{1}H NMR (in MeCN-d_3 and DMSO-d_6) and elemental analysis data.

*Complex [**1·3b**] (First Modification).* Blue-black crystals (22.3 mg, 85% yield): mp 272−279 °C (decomp.); ^{1}H NMR (500.13 MHz, MeCN-d_3, 25 °C) δ 3.47 (br.s, 4H, 2 CH_2NH$_3$), 3.74−3.80 (m, 12H, 6 CH$_2$O), 3.80−3.86 (m, 12H, 6 CH$_2$O), 3.91 (br.m, 4H, 2 3′-CH_2CH$_2$OAr), 3.98 (br.m, 4H, 2 4′-CH_2CH$_2$OAr), 4.12 (br.m, 4H, 2 3′-CH_2OAr), 4.36 (br.m, 4H, 2 4′-CH_2OAr), 4.62 (t, J = 6.5 Hz, 4H, 2 CH$_2$N), 6.93 (s, 2H, CH=CH), 6.95 (br.s, 2H, 2 2′-H), 7.13 (d, J = 8.3 Hz, 2H, 2 5′-H), 7.23 (br.d, J = 8.3 Hz, 2H, 2 6′-H), 7.68 (br.s, 6H, 2 NH$_3$), 8.25 (d, J = 6.3 Hz, 4H, 2 3-H, 2 5-H), 8.37 (br.s, 4H, 2 2-H, 2 6-H) ppm; IR (Nujol) 3165 (N$^+$−H) cm^{-1}. Anal. Calcd. for $C_{34}H_{48}O_{12}\cdot C_{14}H_{22}Cl_4N_4O_{16}\cdot H_2O$: C 43.98, H 5.54, N 4.27. Found: C 43.87, H 5.45, N 4.07.

*Complex [**1·3b**] (Second Modification).* Obtained by recrystallization of the first modification [**1·3b**], a light beige powder (20.2 mg, 92% yield): mp 267−268 °C (decomp.); ^{1}H NMR (500.13 MHz, MeCN-d_3, 25 °C) δ 3.44 (t, J = 6.4 Hz, 4H, 2 CH_2NH$_3$), 3.73−3.80 (m, 12H, 6 CH$_2$O), 3.80−3.87 (m, 12H, 6 CH$_2$O), 3.91 (m, 4H, 2 3′-CH_2CH$_2$OAr), 3.98 (m, 4H, 2 4′-CH_2CH$_2$OAr), 4.11 (m, 4H, 2 3′-CH_2OAr), 4.36 (m, 4H, 2 4′-CH_2OAr), 4.63 (t, J = 6.4 Hz, 4H, 2 CH$_2$N), 6.94 (br.s, 4H, CH=CH, 2 2′-H), 7.13 (d, J = 8.0 Hz, 2H, 2 5′-H), 7.25 (br.d, J = 8.0 Hz, 2H, 2 6′-H), 7.66 (br.s, 6H, 2 NH$_3$), 8.24 (br.s, 4H, 2 3-H, 2 5-H), 8.34 (br.s, 4H, 2 2-H, 2 6-H) ppm; IR (Nujol) 3156 (N$^+$−H) cm^{-1}. Anal. Calcd. for $C_{34}H_{48}O_{12}\cdot C_{14}H_{22}Cl_4N_4O_{16}$: C 44.59, H 5.46, N 4.33. Found: C 44.60, H 5.45, N 4.41.

*Complex [**1·3c**].* Brown crystals (24.3 mg, 91% yield): mp 200−205 °C; ^{1}H NMR (500.13 MHz, MeCN-d_3, 25 °C) δ 1.75 (br.s, 4H, 2 CH_2CH$_2$N), 2.95 (br.s, 4H, 2 CH_2NH$_3$), 3.66−3.86 (m, 24H, 12 CH$_2$O), 3.94 (br.s, 8H, 4 CH_2CH$_2$OAr), 4.16 (br.s, 4H, 2 3′-CH_2OAr), 4.34 (br.s, 4H, 2 4′-CH_2OAr), 4.47 (t, J = 7.8 Hz, 4H, 2 CH$_2$N), 6.84 (br.s, 2H, CH=CH), 6.90 (br.s, 2H, 2 2′-H), 7.08 (br.m, 2H, 2 5′-H), 7.15 (br.s, 2H, 2 6′-H), 7.51 (br.s, 6H, 2 NH$_3$), 8.27 (d, J = 6.5 Hz, 4H, 2 3-H, 2 5-H), 8.46 (d, J = 6.5 Hz, 4H, 2 2-H, 2 6-H) ppm; IR (Nujol) 3178 (N$^+$−H) cm^{-1}. Anal. Calcd. for $C_{34}H_{48}O_{12}\cdot C_{16}H_{26}Cl_4N_4O_{16}\cdot H_2O$: C 44.85, H 5.72, N 4.18. Found: C 44.84, H 5.82, N 4.18.

*Complex [**1·4b**].* Blue-black crystals (21.4 mg, 80% yield): mp >300 °C (decomp.); ^{1}H NMR (500.13 MHz, MeCN-d_3, 50 °C) δ 3.80−3.94 (m, 36H, 2 CH_2NH$_3$, 16 CH$_2$O), 4.03 (br.m, 4H, 2 3′-CH_2OAr), 4.38 (br.s, 4H, 2 4′-CH_2OAr), 5.15 (br.t, J = 6.0 Hz, 4H, 2 CH$_2$N), 6.21 (s, 2H, CH=CH), 6.29 (br.s, 2H, 2 2′-H), 6.98 (br.s, 2H, 2 6′-H), 7.03 (br.s, 2H, 2 5′-H), 7.78 (br.s, 6H, 2 NH$_3$), 8.69 (s, 4H, 4-H, 5-H, 9-H, 10-H), 9.54 (br.s, 4H, 1-H, 3-H, 6-H, 8-H) ppm; IR (Nujol) 3177 (N$^+$−H) cm^{-1}. Anal. Calcd. for $C_{34}H_{48}O_{12}\cdot C_{18}H_{22}Cl_4N_4O_{16}$: C 46.58, H 5.26, N 4.18. Found: C 46.36, H 5.26, N 4.17.

*Complex [**1·4c**].* Blue-black crystals (23.0 mg, 84% yield): mp >300 °C (decomp.); ^{1}H NMR (500.13 MHz, MeCN-d_3, 25 °C) δ 2.01 (br.s, 4H, 2 CH_2CH$_2$N), 3.13 (br.m, 4H, 2 CH_2NH$_3$), 3.73−3.94 (m, 28H, 14 CH$_2$O), 3.98 (br.s, 8H, 2 4′-CH_2CH$_2$OAr, 2 3′-CH_2OAr), 4.40 (br.s, 4H, 2 4′-CH_2OAr), 4.91 (t, J = 7.5 Hz, 4H, 2 CH$_2$N), 5.84 (br.s, 2H, CH=CH), 6.35 (s, 2H, 2 2′-H), 6.62 (br.s, 2H, 2 6′-H), 7.07 (br.s, 2H, 2 5′-H), 7.58 (br.s, 6H, 2 NH$_3$), 8.78 (s, 4H, 4-H, 5-H, 9-H, 10-H), 9.54 (br.s, 4H, 1-H, 3-H, 6-H, 8-H) ppm; IR (Nujol) 3175 (N$^+$−H) cm^{-1}. Anal. Calcd. for $C_{34}H_{48}O_{12}\cdot C_{20}H_{26}Cl_4N_4O_{16}$: C 47.38, H 5.45, N 4.09. Found: C 47.29, H 5.57, N 4.05.

Spectrophotometry. The CT absorption spectra of pure **D·A** and **D·A·D** complexes in MeCN (extra pure grade, water content <0.03%), as well as the complex formation constants K_1 and K_2, were derived from global analysis of spectrophotometric titration data, as described previously for the **1**/**2c** system.[6b] Spectrophotometric titrations were conducted in 1 or 5 cm quartz cells with ground-in stoppers. All manipulations with solutions were performed in a darkroom under red light because bis(crown)stilbene **1** underwent photoisomerization under daylight.

A competitive titration method was applied to assess the formation constants K_1 for the **D·A** complexes. The competing reactants were 1,8-diammoniooctane diperchlorate[18] (with **3b** and **4b**) and 1,10-diammoniodecane diperchlorate[19] (with **3c** and **4c**). The complex formation constants for the diammonioalkane salts with **1** in MeCN are known from ref 6b. The concentration of the competing reactant was maintained at 1 × 10^{-3} M. With **3b,c**, the concentrations of **1** were maintained at 4 × 10^{-5} M, and the concentration of **3b,c** was varied from 0 to 4 × 10^{-4} M. With **4b,c**, the concentration of **1** was varied from 0 to 4 × 10^{-4} M, and the concentration of **4b,c** was maintained at 4 × 10^{-5} M. The competitive titration data are shown in Figures S29−S32 (Supporting Information).

The formation constants K_2 for the **D·A·D** complexes were derived from direct titration experiments: the concentration of acceptor was maintained at 5 × 10^{-4} M (**3b,c**) or at 2 × 10^{-4} M (**4b,c**), and the concentration of **1** was varied from 0 to 0.05 M. The direct titration data are shown in Figures S33−S36 (Supporting Information).

Fluorescence Studies. Experiments were conducted in MeCN at ambient temperature in 1 cm quartz cells; the atmospheric oxygen contained in solutions was not removed. Fluorescence spectra were corrected, taking into account the spectral sensitivity of the photomultiplier tube. The fluorescence quantum yield of **4c** in MeCN (excitation at 340 nm) was determined using anthracene in ethanol as the standard.[20] Fluorometric titrations of [**1·4c**] with metal perchlorates were performed using a stock solution of complex [**1·4c**], as prepared by dissolving a crystalline sample.

Cyclic Voltammetry. Cyclic voltammetry experiments were carried out using a three-electrode system. A glassy carbon disk (d = 1.8 mm) was used as the working electrode. The reference electrode was Ag|AgCl|KCl (aq., sat.). A platinum plate (S = 0.5 cm^2) served as the auxiliary electrode. Cyclic voltammograms were measured in MeCN solutions in the presence of Bu_4NClO_4 (0.1 M) at 22 °C. All solutions were deaerated by argon purging. The potential scanning rate was 200 mV/s. Ferrocene (1 mM) was used as the internal reference. The concentrations of reactants were 1 mM.

^{1}H NMR Titration. Experiments were conducted in MeCN-d_3 (water content <0.05%) at 25 ± 1 °C. The formation constants K_1

dx.doi.org/10.1021/jo201172w |*J. Org. Chem.* 2011, 76, 6768–6779

for the [**1**·**3**(**4**)**a**] complexes and K_2 for the [**1**·**3**(**4**)**b**,**c**·**1**] complexes were derived from direct titration experiments; the concentration of acceptor (C_A) was maintained at 1×10^{-3} M and the concentration of **1** (C_D) was varied from 0 to $(6-20) \times 10^{-3}$ M (**3b**,**c**, **4b**,**c**) or to 0.04 M (**3a**, **4a**). For systems **1**/**2**(**3**,**4**)**b**,**c**, the dependencies of $\Delta\delta_H$ on C_D/C_A measured at $C_D > C_A$ were described well by the simplified complexation model taking into account only eq 2, which allowed us to assess the formation constants K_2 for termolecular complexes [**1**·**3**(**4**)**b**,**c**·**1**]. The use of this model is justified by the fact that when $C_D > C_A$, the partial concentrations of uncomplexed acceptors **3**(**4**)**b**,**c** are negligibly low due to very high values of the formation constants K_1 for the bimolecular complexes [**1**·**3**(**4**)**b**,**c**].

Competitive ^{1}H NMR titration was applied to measure the formation constants K_1 for the [**1**·**2**(**3**,**4**)**b**,**c**] complexes. The concentrations of **2**(**3**,**4**)**b**,**c** and **1** were maintained at 1×10^{-3} and 1.2×10^{-3} M, respectively, and the concentration of the competing reagent, 1,10-diammoniodecane diperchlorate, was varied from 0 to $(1.0-1.3) \times 10^{-2}$ M.

The complex formation constants were calculated using the HYPNMR program.[21]

X-ray Crystal Structure Determinations, Crystal Data. *Data for* ***3c***·*2H*$_2$*O.* $C_{16}H_{30}Cl_4N_4O_{18}$, monoclinic, $P2_1/n$, a = 12.3277(5), b = 8.9364(4), c = 13.1357(6) Å, β = 104.0710(10)°, V = 1403.68(11) Å^3, Z = 2, μ = 0.510 mm^{-1}, F_{000} = 732. T = 120.0(2) K, θ range 2.03−29.00°. Index ranges h, k, l (indep set): −16 to 16, −12 to 11, −17 to 17. Reflections measd: 14828, indep: 3736 [R_{int} = 0.0162], obsvd [$I > 2\sigma(I)$]: 3385. Final R indices [$I > 2\sigma(I)$]: R_1 = 0.0305, wR_2 = 0.0849, GOF = 1.079.

Data for ***4a***. $C_{18}H_{18}Cl_2N_2O_8$, monoclinic, $P2_1/c$, a = 5.8449(13), b = 13.893(3), c = 11.655(3) Å, β = 94.210(4)°, V = 943.8(4) Å^3, Z = 2, μ = 0.397 mm^{-1}, F_{000} = 476. T = 170(2) K, θ range 2.28−29.00°. Index ranges h, k, l (indep set): −7 to 7, −18 to 18, −15 to 15. Reflections measd: 7651, indep: 2441 [R_{int} = 0.0429], obsvd [$I > 2\sigma(I)$]: 1766. Final R indices [$I > 2\sigma(I)$]: R_1 = 0.0575, wR_2 = 0.1813, GOF = 1.097.

Data for [***1***·***3b***]·*C*$_4$*H*$_8$*O*$_2$·*3H*$_2$*O.* $C_{52}H_{84}Cl_4N_4O_{33}$, triclinic, $P\bar{1}$, a = 8.7194(7), b = 11.7380(10), c = 17.3124(15) Å, α = 79.194(4), β = 80.249(3), γ = 77.874(3)°, V = 1686.0(2) Å^3, Z = 1, μ = 0.268 mm^{-1}, F_{000} = 756. T = 120.0(2) K, θ range 2.41−25.00°. Index ranges h, k, l (indep set): −10 to 10, −13 to 8, −19 to 20. Reflections measd: 7340, indep: 5564 [R_{int} = 0.0457], obsvd [$I > 2\sigma(I)$]: 3170. Final R indices [$I > 2\sigma(I)$]: R_1 = 0.1138, wR_2 = 0.2706, GOF = 1.026.

Data for [***1***·***3c***]·*0.25MeCN*·*0.44H*$_2$*O.* $C_{50.5}H_{75.63}Cl_4N_{4.25}O_{28.44}$, monoclinic, $P2_1/n$, a = 20.790(3), b = 27.460(4), c = 21.875(3) Å, β = 90.096(4)°, V = 12488(3) Å^3, Z = 8, μ = 0.279 mm^{-1}, F_{000} = 5631. T = 120.0(2) K, θ range 0.74−27.54°. Index ranges h, k, l (indep set): −27 to 27, −35 to 35, −28 to 18. Reflections measd: 87 572, indep: 28 695 [R_{int} = 0.0798], obsvd [$I > 2\sigma(I)$]: 14199. Final R indices [$I > 2\sigma(I)$]: R_1 = 0.0715, wR_2 = 0.1694, GOF = 0.875.

The single crystals of all compounds were coated with perfluorinated oil and mounted on a diffractometer [graphite monochromatized Mo−K$_\alpha$ radiation (λ = 0.71073 Å), ω scan mode] under a stream of cold nitrogen. The sets of experimental reflections were measured and the structures were solved by direct methods and refined by full matrix least-squares methods against F^2 with anisotropic thermal parameters for all non-hydrogen atoms (except for atoms of the strongly disordered anion Cl(2)O$_4^-$ and solvation dioxane and water molecules in structure [**1**·**3b**]·C$_4$H$_8$O$_2$·3H$_2$O, which were refined isotropically). In some cases, absorption correction was applied using the SADABS method. The hydrogen atoms were fixed at calculated positions at carbon atoms and then refined with the isotropic approximation for **3c**·2H$_2$O and **4a** or by using a riding model for the other structures. The hydrogen atoms of NH_3^+ groups were calculated geometrically and then refined isotropically (with mild restraints for N−H bond distances). The hydrogen atoms of the solvation water molecule in structure **3c**·2H$_2$O were located from the difference Fourier map and refined isotropically. In other structures, hydrogen atoms of the solvation water molecules were not located. All the calculations were performed using the SHELXTL-Plus software.[22]

CCDC 831395 (**3c**·2H$_2$O), 831396 (**4a**), 831394 ([**1**·**3c**]·0.25MeCN·0.44H$_2$O), and 831393 ([**1**·**3b**]·C$_4$H$_8$O$_2$·3H$_2$O) contain supplementary crystallographic data for this paper. These data can be obtained free of charge from the Cambridge Crystallographic Data Center via www.ccdc.cam.ac.uk/data_request/cif.

Quantum-Chemical Calculations. Geometries of the acceptor molecules **2**−**4** in MeCN were calculated by RI-DFT method using the PBE functional[23] and the def2-TZVP(-f) basis set.[24] The geometries were fully optimized using the ORCA program.[25] The solvent was simulated using the COSMO method as implemented in ORCA.[26]

■ ASSOCIATED CONTENT

Ⓢ Supporting Information. ^{1}H and ^{13}C NMR, HSQC, NOESY spectra, absorption and fluorescence spectra, cyclic voltammograms, X-ray crystallographic data, and molecular modeling details. This material is available free of charge via the Internet at http://pubs.acs.org.

■ AUTHOR INFORMATION

Corresponding Author
*E-mail: spgromov@mail.ru.

■ ACKNOWLEDGMENT

Financial support from the Russian Foundation for Basic Research, the Russian Academy of Sciences, and the Royal Society of Chemistry is gratefully acknowledged.

■ REFERENCES

(1) (a) Föster, R. *Organic Charge-Transfer Complexes*; Academic Press: New York, 1969. (b) Mataga, N.; Kubota, T. *Molecular Interactions and Electronic Spectra*; Marcel Dekker: New York, 1970. (c) Rosokha, S. V.; Kochi, J. K. *Acc. Chem. Res.* **2008**, *41*, 641.

(2) (a) Odell, B.; Reddington, M. V.; Slawin, A. M. Z.; Spencer, N.; Stoddart, J. F.; Williams, D. J. *Angew. Chem., Int. Ed.* **1988**, *27*, 1547. (b) Amabilino, D. B.; Stoddart, J. F. *Chem. Rev.* **1995**, *95*, 2725. (c) Ballardini, R.; Balzani, V.; Credi, A.; Gandolfi, M. T.; Langford, S. J.; Menzer, S.; Prodi, L.; Stoddart, J. F.; Venturi, M.; Williams, D. J. *Angew. Chem., Int. Ed.* **1996**, *35*, 978. (d) Koshkakaryan, G.; Klivansky, L. M.; Cao, D.; Snauko, M.; Teat, S. J.; Struppe, J. O.; Liu, Y. *J. Am. Chem. Soc.* **2009**, *131*, 2078.

(3) (a) Slifkin, M. A. *Charge-Transfer Interactions in Biomolecules*; Academic Press: London, 1971. (b) Gutmann, F.; Johnson, C.; Keyzer, H.; Molnar, J. *Charge Transfer Complexes in Biological Systems*; Marcel Dekker: New York, 1997.

(4) (a) Shirota, Y.; Kageyama, H. *Chem. Rev.* **2007**, *107*, 953. (b) Günes, S.; Neugebauer, H.; Sariciftci, N. S. *Chem. Rev.* **2007**, *107*, 1324. (c) Mori, T. *Chem. Lett.* **2011**, *40*, 428.

(5) (a) Thomas, S. W., III; Joly, G. D.; Swager, T. M. *Chem. Rev.* **2007**, *107*, 1339. (b) D'Souza, F.; Ito, O. *Chem. Commun.* **2009**, 4913.

(6) (a) Gromov, S. P.; Ushakov, E. N.; Vedernikov, A. I.; Lobova, N. A.; Alfimov, M. V.; Strelenko, Yu. A.; Whitesell, J. K.; Fox, M. A. *Org. Lett.* **1999**, *1*, 1697. (b) Ushakov, E. N.; Gromov, S. P.; Vedernikov, A. I.; Malysheva, E. V.; Botsmanova, A. A.; Alfimov, M. V.; Eliasson, B.; Edlund, U. G.; Whitesell, J. K.; Fox, M. A. *J. Phys. Chem. A* **2002**, *106*, 2020.

(7) Ushakov, E. N.; Nadtochenko, V. A.; Gromov, S. P.; Vedernikov, A. I.; Lobova, N. A.; Alfimov, M. V.; Gostev, F. E.; Petrukhin, A. N.; Sarkisov, O. M. *Chem. Phys.* **2004**, *298*, 251.

(8) Vedernikov, A. I.; Basok, S. S.; Gromov, S. P.; Kuz'mina, L. G.; Avakyan, V. G.; Lobova, N. A.; Kulygina, E. Yu.; Titkov, T. V.; Strelenko, Yu. A.; Ivanov, E. I.; Howard, J. A. K.; Alfimov, M. V. *Russ. J. Org. Chem.* **2005**, *41*, 843.

(9) (a) Kuz'mina, L. G.; Churakov, A. V.; Howard, J. A. K.; Vedernikov, A. I.; Lobova, N. A.; Botsmanova, A. A.; Alfimov, M. V.; Gromov, S. P. *Crystallogr. Rep.* **2005**, *50*, 234. (b) Gromov, S. P.; Vedernikov, A. I.; Ushakov, E. N.; Lobova, N. A.; Botsmanova, A. A.; Kuz'mina, L. G.; Churakov, A. V.; Strelenko, Yu. A.; Alfimov, M. V.; Howard, J. A. K.; Johnels, D.; Edlund, U. G. *New J. Chem.* **2005**, *29*, 881.

(10) Britt, B. M.; McHale, J. L. *Chem. Phys. Lett.* **1997**, *270*, 551.

(11) Butin, K. P.; Moiseeva, A. A.; Gromov, S. P.; Vedernikov, A. I.; Botsmanova, A. A.; Ushakov, E. N.; Alfimov, M. V. *J. Electroanal. Chem.* **2003**, *547*, 93.

(12) (a) Yasuda, A.; Mori, H.; Seto, J. *J. Appl. Electrochem.* **1987**, *17*, 567. (b) Kaifer, A. E. *Acc. Chem. Res.* **1999**, *32*, 62.

(13) (a) Credi, A.; Dumas, S.; Silvi, S.; Venturi, M.; Arduini, A.; Pochini, A.; Secchi, A. *J. Org. Chem.* **2004**, *69*, 5881. (b) Guo, D.-S.; Wang, L.-H.; Liu, Y. *J. Org. Chem.* **2007**, *72*, 7775.

(14) (a) Ong, W.; Gómez-Kaifer, M.; Kaifer, A. E. *Org. Lett.* **2002**, *4*, 1791. (b) Jeon, W. S.; Kim, H.-J.; Lee, C.; Kim, K. *Chem. Commun.* **2002**, 1828. (c) Ko, Y. H.; Kim, E.; Hwang, I.; Kim, K. *Chem. Commun.* **2007**, 1305.

(15) Balzani, V.; Bandmann, H.; Ceroni, P.; Giansante, C.; Hahn, U.; Klärner, F.-G.; Müller, U.; Müller, W. M.; Verhaelen, C.; Vicinelli, V.; Vögtle, F. *J. Am. Chem. Soc.* **2006**, *128*, 637.

(16) (a) Devonport, W.; Blower, M. A.; Bryce, M. R.; Goldenberg, L. M. *J. Org. Chem.* **1997**, *62*, 885. (b) Ballardini, R.; Balzani, V.; Clemente-León, M.; Credi, A.; Gandolfi, M. T.; Ishow, E.; Perkins, J.; Stoddart, J. F.; Tseng, H.-R.; Wenger, S. *J. Am. Chem. Soc.* **2002**, *124*, 12786. (c) Lestini, E.; Nikitin, K.; Müller-Bunz, H.; Fitzmaurice, D. *Chem.—Eur. J.* **2008**, *14*, 1095.

(17) Hünig, S.; Groβ, J.; Lier, E. F.; Quast, H. *Liebigs Ann.* **1973**, 339.

(18) Gromov, S. P.; Vedernikov, A. I.; Kuz'mina, L. G.; Lobova, N. A.; Basok, S. S.; Strelenko, Yu. A.; Alfimov, M. V. *Russ. Chem. Bull., Int. Ed.* **2009**, *58*, 108.

(19) Vedernikov, A. I.; Kuz'mina, L. G.; Botsmanova, A. A.; Strelenko, Yu. A.; Howard, J. A. K.; Alfimov, M. V.; Gromov, S. P. *Mendeleev Commun.* **2007**, *17*, 148.

(20) Suzuki, K.; Kobayashi, A.; Kaneko, S.; Takehira, K.; Yoshihara, T.; Ishida, H.; Shiina, Y.; Oishi, S.; Tobita, S. *Phys. Chem. Chem. Phys.* **2009**, *11*, 9850.

(21) Frassineti, C.; Ghelli, S.; Gans, P.; Sabatini, A.; Moruzzi, M. S.; Vacca, A. *Anal. Biochem.* **1995**, *231*, 374.

(22) *SHELXTL-Plus*, Version 5.10; Bruker AXS Inc.: Madison, WI, 1997.

(23) Perdew, J. P.; Burke, K.; Ernzerhof, M. *Phys. Rev. Lett.* **1996**, *77*, 3865.

(24) Weigend, F.; Ahlrichs, R. *Phys. Chem. Chem. Phys.* **2005**, *7*, 3297.

(25) Neese, F. *OCRA — An Ab Initio, DFT and Semiempirical Electronic Structure Package*, Version 2.8; Universität Bonn: Bonn, Germany, 2010.

(26) Sinnecker, S.; Rajendran, A.; Klamt, A.; Diedenhofen, M.; Neese, F. *J. Phys. Chem. A* **2006**, *110*, 2235.